

## Multinucleon transfer reactions in $^{32}\text{S}+^{208}\text{Pb}$ close to the Coulomb barrier

L. Corradi,<sup>1</sup> A. M. Stefanini,<sup>1</sup> D. Ackermann,<sup>1</sup> S. Beghini,<sup>2</sup> G. Montagnoli,<sup>2</sup> C. Petrache,<sup>3</sup> F. Scarlassara,<sup>2</sup> C. H. Dasso,<sup>4,6</sup> G. Pollarolo,<sup>5</sup> and A. Winther<sup>4</sup>

<sup>1</sup>*Instituto Nazionale di Fisica Nucleare-Laboratori Nazionali di Legnaro, I-35020 Legnaro, Italy*

<sup>2</sup>*Instituto Nazionale di Fisica Nucleare and Dipartimento di Fisica dell'Università, I-35131 Padova, Italy*

<sup>3</sup>*Institute of Physics and Nuclear Engineering, Bucharest, Romania*

<sup>4</sup>*The Niels Bohr Institute, Blegdamsvej 17, 2100 Copenhagen Ø, Denmark*

<sup>5</sup>*Instituto Nazionale di Fisica Nucleare and Dipartimento di Fisica Teorica dell'Università, Torino, Italy*

<sup>6</sup>*Sektion Physik der Universität München, D-85748, Garching, Germany*

(Received 25 January 1994)

Elastic scattering and transfer reactions for the system  $^{32}\text{S}+^{208}\text{Pb}$  have been measured at the laboratory energy of 173.4 MeV.  $Q$ -value distributions and angle differential cross sections have been obtained for a variety of transfer channels. The experimental results for the different charge and mass partitions are analyzed in terms of multiple single-particle and pair-correlated transfer processes.

PACS number(s): 25.70.Bc, 25.70.Hi, 25.70.Pq

Elastic, inelastic, and transfer reactions provide important information for the description of several phenomena occurring in collisions between heavy ions and are especially important at energies close to the Coulomb barrier [1]. In particular, multinucleon transfer processes yield valuable information about pairing correlations in nuclei [2–4], the transition from the quasielastic to the deep-inelastic regime [5,7], and the energy dependence of fusion cross sections [8–13]. Thanks to the improvement of high-resolution experimental setups some multinucleon transfer data have recently become available [10–17], but are still too scarce to delineate a consistent systematic. Moreover, and most important, a theoretical microscopic description of situations involving complex transfer reactions is still lacking. Reliable calculations can only be made for the transfer of one nucleon [by using, e.g., distorted-wave Born approximation (DWBA) or a coupled-channel formalism [18,19]]. For cases where many nucleons are involved, mostly semiphenomenological approaches have been used until now [5,15].

In this Rapid Communication we report on the results of an experiment whose main aim was to investigate the multinucleon transfer processes for the system  $^{32}\text{S}+^{208}\text{Pb}$  at bombarding energies close to the Coulomb barrier. Extensive data on heavy-ion reactions with lead as the target already exist (see [14] and references therein), but we have tried in this work to perform a measurement as complete as possible of the one and many-nucleon transfer channels as well as of the elastic scattering. A combination of spherical nuclei was chosen in order to perform easier and more reliable calculations. The double-magic lead nucleus is, from this point of view, an ideal candidate. Moreover, being its first excited level at an excitation energy of 2.62 MeV and that of sulphur at 2.23 MeV, the resolution of our detector makes it possible to isolate pure elastic scattering events. This allows, in turn, determining quite safely the nuclear potential parameters to be used in the transfer calculations. In these, a microscopic formalism was applied which reproduces the main features of the angular and  $Q$ -value distributions for the numerous transfer channels observed in the ex-

periment. The same system was recently studied with a high-resolution  $\gamma$ -particle coincidence setup, and the population strength of individual levels near the ground state of the transfer products has been investigated [20].

The present experiment was performed at the XTU tandem accelerator of the Laboratori Nazionali di Legnaro. A  $^{32}\text{S}$  beam with intensity of  $\simeq 10$  pA was delivered at an energy of 173.4 MeV (referred to the center of the target), corresponding to 1.01 times the nominal Coulomb barrier [21]. A  $^{208}\text{Pb}$  target with a thickness of  $200 \mu\text{g}/\text{cm}^2$  was placed inside a sliding-seal scattering chamber; this was connected to a time-of-flight system consisting of two microchannel-plate detectors and a  $\Delta E-E_{\text{res}}$  position-sensitive ionization chamber, giving good mass, charge, and  $Q$ -value resolutions. A full description of the setup can be found in a previous paper [12]. Two silicon detectors were placed at  $\pm 15^\circ$  with respect to the beam line for the relative normalization of different runs. Angular distributions were measured from  $30^\circ$  to  $135^\circ$  in the laboratory system, covering most of the total transfer flux.

The good energy resolution of the ionization chamber allowed, by a careful fit procedure, discriminating pure elastic scattering from inelastic events. Only at the most backward angles the big intensity of the inelastic channels and the low statistics introduce large errors (up to 30%). Figure 1 shows examples of mass and  $Q$ -value spectra obtained with a software gate on the nuclear charge  $Z=16$ . The  $Q$ -value distribution was produced with a further gate on mass  $A=32$  and a correction procedure that eliminates a tail in the total energy spectra, due to field inhomogeneities of the chamber. To this end, position information was used which also reduces the kinematic shift effects.

The angular distribution for elastic scattering is shown in Fig. 2 (left-hand side), where the points at the most forward angles have been normalized to the Rutherford cross section. The full line is the result of a coupled-channel calculation [22] made by coupling the elastic channel to the first quadrupole ( $E_{2^+}=2.23$  MeV,  $\beta_2=0.27$ ) and octupole ( $E_{3^-}=2.62$  MeV,  $\beta_3=0.094$ ) ex-

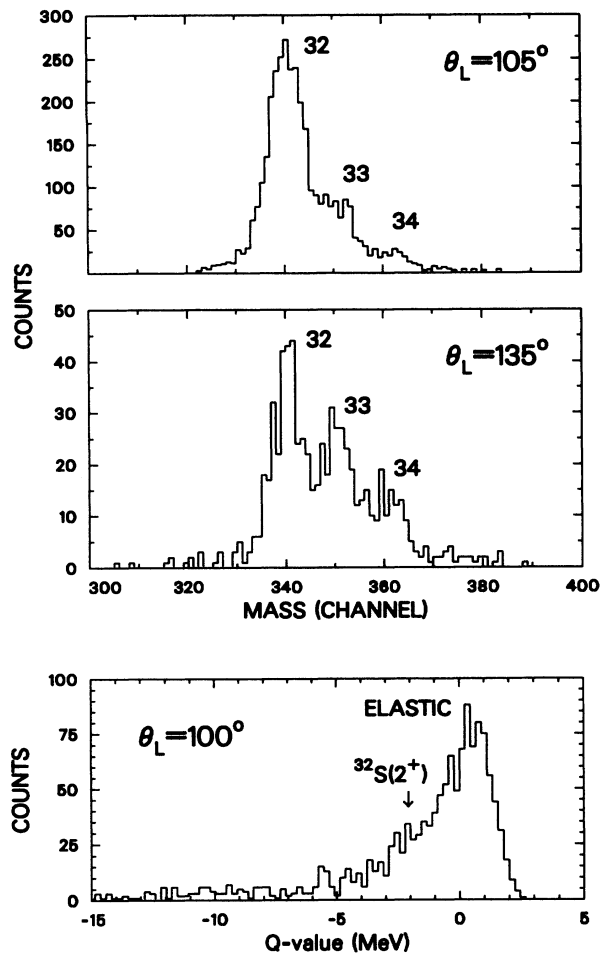


FIG. 1. Experimental mass and  $Q$ -value spectra obtained at the indicated laboratory angles (see text for details).

cited states of  $^{32}\text{S}$  and  $^{208}\text{Pb}$ , respectively. The nuclear potential ( $V_0 = -85$  MeV,  $W_0 = -50$  MeV,  $r_0^R = r_0^I = 1.18$  fm and  $a^R = a^I = 0.68$  fm) was obtained with a best-fit procedure starting from the real empirical potential of Ref. [23], keeping for the imaginary part the same geometry and searching for  $V_0$  and  $W_0$ . This procedure leads to a potential that is about 7% more attractive

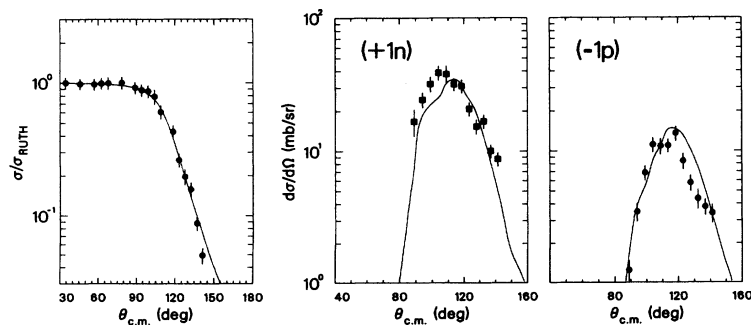


FIG. 2. The elastic angular distribution is shown in the left-hand side in comparison with the coupled-channel calculation (full line). The neutron pickup ( $+1n$ ) and the proton stripping ( $-1p$ ) angular distributions are shown on the right-hand side in comparison with the complex WKB calculations as explained in the text.

than the one given in [23].

In the following we perform an analysis of the reaction processes based on the same approximations which were successfully exploited to calculate the absorptive [26,27] and polarization [28] component of the optical potential and the off-diagonal inelastic couplings [29]. We start the analysis of the transfer data from the one-neutron pick-up ( $+1n$ ) and one-proton stripping ( $-1p$ ) channels.<sup>1</sup> Following previous work [24] we analyze these data with complex WKB theory [25], which is adequate both below and above the Coulomb barrier. In this approximation the cross section for one-particle transfer can be written in the form

$$\left[ \frac{d\sigma}{d\Omega} \right]_{\text{tr}} = \sum_{a_i, a_f, \lambda} \frac{\kappa_f}{\kappa_i} \left| \sum_{l\mu} \frac{2l+1}{2i\kappa} c_{a_f a_i}^{\lambda\mu}(l) T(l) P_l(\cos\theta) \right|^2, \quad (1)$$

where, for the partial wave  $l$ ,  $c_{a_f a_i}^{\lambda\mu}(l)$  is the first-order semiclassical amplitude for the transition from the single-particle level  $a_i \equiv (n_i, l_i, j_i)$  to the single-particle level  $a_f$  and where  $T(l)$  is the  $T$  matrix for elastic scattering related to the nuclear ( $\delta_N$ ) and Coulomb ( $\delta_C$ ) phase shifts

$$T(l) = e^{2i[\delta_N(l) + \delta_C(l)]}. \quad (2)$$

The sum in (1) has to be performed over all the single-particle levels of both reaction partners, since the experiment does not discriminate individual transitions. The semiclassical amplitudes  $c_{a_f a_i}^{\lambda\mu}(l)$  are evaluated in the complex WKB approximation by utilizing the single-particle form factors of Refs. [26,27]. For more details see Ref. [24].

Employing all the known single-particle levels of target and projectile reported in Table I and their corresponding spectroscopic factors one obtains the results shown in Fig. 2 (right-hand side). To calculate the  $T$  matrix  $T(l)$  we have used the nuclear potential obtained from the calculation discussed above.

Figure 3 shows the  $Q$ -integrated angular distributions for almost all the transfer channels identified in the experiment. The cross sections were obtained by integrating

<sup>1</sup>Only neutron pickup and proton stripping processes need be considered since the other single-nucleon transfer channels are widely off the optimum  $Q$  value and are not observed in the present experiment.

TABLE I. Single-particle levels of projectile and target used in the calculation. The Fermi energy for neutrons is after the first three levels of  $^{32}\text{S}$  and after the first seven levels of  $^{208}\text{Pb}$ , whereas for protons it lies after the first level of  $^{32}\text{S}$  and after the first six levels of  $^{208}\text{Pb}$ .

	$(n, l, j)_n$	B.E. (MeV)	$U^2(V^2)$	$(n, l, j)_p$	B.E. (MeV)	$U^2(V^2)$
$^{32}\text{S}$	1f5/2	-3.74	1.000	1d3/2	-2.28	1.000
	2p3/2	-5.42	0.875	2s1/2	-8.86	0.782
	1f7/2	-5.71	0.530	1d3/2	-10.13	0.831
	2s1/2	-7.79	0.325	1d5/2	-11.10	1.000
	1d3/2	-8.64	0.875			
	2s1/2	-15.08	1.000			
	1d5/2	-17.31	1.000			
	1p1/2	-24.67	1.000			
$^{208}\text{Pb}$	3d3/2	-1.40	1.000	1p1/2	-0.17	1.000
	2g3/2	-1.45	1.000	3p3/2	-0.68	1.000
	4s1/2	-1.91	1.000	2f5/2	-0.98	1.000
	3d5/2	-2.37	1.000	1i9/2	-2.19	1.000
	1j15/2	-2.51	1.000	2f7/2	-2.90	1.000
	1i11/2	-3.16	1.000	1h9/2	-3.80	1.000
	2g9/2	-3.94	1.000	1d3/2	-8.37	1.000
	3p1/2	-7.37	1.000	1h11/2	-9.36	1.000
	2f5/2	-7.94	1.000	2d5/2	-9.69	1.000
	3p3/2	-8.27	1.000	1g7/2	-11.49	1.000
	1i13/2	-9.00	1.000	1g9/2	-14.61	1.000
	2f7/2	-9.71	1.000	2p1/2	-14.96	1.000
	1h9/2	-10.78	1.000	2p3/2	-15.88	1.000
	1h11/2	-14.58	1.000			
	3s1/2	-14.89	1.000			

over the whole observed  $Q$ -value interval. Beyond the “usual” pickup of neutrons ( $+xn$ ) and stripping of protons ( $-xp$ ), the presence of complex channels like single and double “charge-exchange” ( $-1p + 1n, -2p + 2n$ ) and still more complicated configurations ( $-1p + 2n, -1p + 3n$ , etc.) is noteworthy. The angular distributions are in almost all cases bell-shaped, underlying the grazing character of the reactions; under these conditions it is possible to describe the complicate multiple-transfer channels in terms of single-nucleon stripping and pickup reactions [6,7].

When the two ions are brought in close contact many single-particle transfer transitions ( $a_i \rightarrow a_f$ ) become open and take place simultaneously with the collective excitation of inelastic and pair-transfer modes. Although there are cross couplings among all these elementary processes their effect is relatively unimportant in the grazing regime. Here the probability for each individual transition is rather small and all these reaction channels can be considered as independent modes of excitation.

In this approximation the probability for  $n_{fi} (= 0, 1)$  transitions of type  $fi$  (i.e.,  $a_i \rightarrow a_f$ ) can be written as

$$p_{fi}(n_{fi}, l) = \begin{cases} p_{fi}(l) & \text{for } n_{fi} = 1, \\ 1 - p_{fi}(l) & \text{for } n_{fi} = 0, \end{cases} \quad (3)$$

where

$$p_{fi}(l) = \sum_{\lambda\mu} \left| c_{a_f a_i}^{\lambda\mu}(l) \right|^2. \quad (4)$$

The amplitude  $c_{a_f a_i}^{\lambda\mu}(l)$  is here evaluated in first-order perturbation theory as in (1). For independent excitations the probability that a given member of the ensemble  $\{n_{fi}\}$  of transitions (involving different single-particle orbitals  $fi$ ) occurs is given by

$$p(\{n_{fi}\}, l) = \prod_{fi} p_{fi}(n_{fi}, l). \quad (5)$$

With these expressions the probability of generating a given charge transfer  $\Delta Z$  can be calculated via a Monte Carlo procedure where, for each  $l$ , the family of sequences  $\{n_{fi}\}$  leading to that particular value  $\Delta Z$  is statistically sampled. Thus,

$$P(\Delta Z, l) = \sum_{\text{all}\{n_{fi}\}} \delta(\Delta Z - \sum_{i,f} n_{fi} \delta z_{fi}) p(\{n_{fi}\}, l), \quad (6)$$

where  $\delta z_{fi}$  is the charge “quanta” pertinent to the transition  $a_i \rightarrow a_f$ . For proton stripping  $\delta z_{fi} = -1$  while for proton pickup  $\delta z_{fi} = +1$ . The corresponding angular distribution is constructed using

$$\left[ \frac{d\sigma}{d\Omega} \right]_{\Delta Z} = \frac{\kappa_f}{\kappa_i} \left| \sum_l \frac{2l+1}{2i\kappa} \sqrt{P(\Delta Z, l)} e^{i\phi(T(l))} P_l(\cos \theta) \right|^2. \quad (7)$$

where  $\phi(T(l))$  is the phase of the  $T$  matrix in Eq. (1), calculated in the WKB approximation for the average trajectory [24] between initial and final channels. In a similar way one may construct the probabilities and the

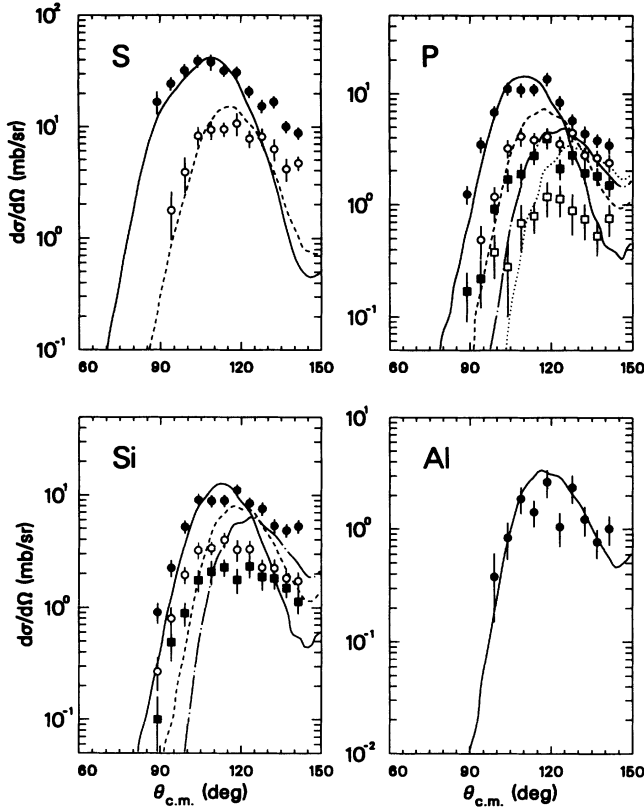


FIG. 3. Angular distributions for all the measured transfer channels. In each frame we have plotted the cross sections corresponding to the different isotopes of the indicated element in comparison with the theoretical calculations. The full circles (full lines) correspond to  $^{33}\text{S}$ ,  $^{31}\text{P}$ ,  $^{30}\text{Si}$ , and  $^{29}\text{Al}$ , the open circles (dashed lines) to  $^{34}\text{S}$ ,  $^{32}\text{P}$ , and  $^{31}\text{Si}$ , the full squares (long dashed-dot lines) to  $^{33}\text{P}$  and  $^{32}\text{Si}$  while the open squares (dotted line) correspond to the  $^{34}\text{P}$ .

cross sections for all other relevant quantities, such as  $\Delta M$ ,  $E_{\text{loss}}$ ,  $E_a^*$ , ... specifying the exit channel.

Equation (5) describes the population of multiple-particle transfer channels like  $+2n$ ,  $-2p$ ,  $+2n - 1p$ , ... via a succession of independent single-particle transition steps. However, the spatial correlation of pairs is expected to give an increase in the transfer of two nucleons, which we may estimate using the macroscopic prescrip-

tion of Ref. [30]. Here the pair transfer couplings are of the form

$$F_P(r) = \beta_P \frac{\partial V(r)}{\partial A} \simeq \left( \frac{\beta_P R}{3A} \right) \frac{\partial V(r)}{\partial r}, \quad (8)$$

where the pair-deformation parameter  $\beta_P$  gives a measure of the correlation strength. To obtain the results shown in Fig. 3 we used  $\beta_P(n) = 25$  and  $\beta_P(p) = 30$ . These values correspond to an effective enhancement factor [2] of about 5 for both proton and neutron pair-transfer channels.

In Fig. 4 we show, for various exit channels, the calculated  $Q$ -value spectra (hatched histograms) for the grazing partial wave  $l = 40$ . This partial wave corresponds approximately to a scattering angle  $\theta_{\text{c.m.}} = 110^\circ$  and we have here compared the calculated spectra with the measured ones (open histograms) using a comparable energy bin. Apart from the channels where the pair-proton transfer plays a role the agreement is quite good, suggesting that the configuration space we are using for neutrons is quite adequate. For the  $-2p$  channel we underestimate the  $Q$  window considerably; perhaps one should add transitions to the continuum (this need is not apparent from the  $-1p$  channel) or, more simply, one should include several proton pair modes at different  $Q$  values. In the shown cross sections, to keep the parameters at a minimum, we used only one pair mode at a  $Q$  value of  $-16$  MeV. Remember that the macroscopic form factor (8) has been tested [30] only for ground-state transitions. Since these inclusive reactions contain also transitions to excited states one should feel free to modify the slope of the form factor. This is also demanded by the angular distribution in Fig. 3.

From the spectra one sees that the transfer proceeds via large  $Q$  values so that the reaction products are produced at high excitation energies. The subsequent nucleon evaporation may influence the cross sections. To investigate this problem we have calculated the excitation energy spectra for the projectilelike and targetlike fragments. At this bombarding energy and in all cases the excitation energy for the light partner is below the neutron and proton separation energy so a direct comparison between the calculated cross section and the

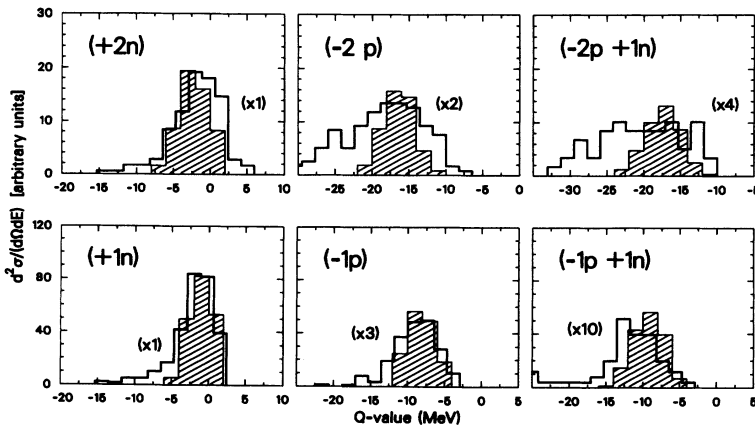


FIG. 4. The  $Q$ -value spectra at  $\theta_{\text{c.m.}} = 110^\circ$  are shown for the indicated channels in comparison with the theoretical histograms (hatched) calculated for the grazing partial wave  $l=40$ . To be able to place the different histograms on the same scale we multiplied the counts for the number quoted in parentheses. The theoretical ones have been normalized arbitrarily.

measured one is possible.

We have measured the elastic scattering and transfer reactions at an energy close to the Coulomb barrier for the system  $^{32}\text{S}+^{208}\text{Pb}$ . The elastic scattering data were compared with a coupled-channel calculation and the inferred nuclear potential parameters were then used for the transfer calculations. On the basis of the good agreement obtained between experimental and theoretical angular distributions for the  $(+1n)$  and  $(-1p)$  channels, a simple model was then applied that reproduces the main features of the more complex multiple-transfer channels. Although discrepancies are evident for some of them the

overall comparison with the data is quite satisfactory. Also the calculated  $Q$ -value distributions show a general good agreement with the experimental data, confirming that in the grazing regime it is possible to generate considerable energy losses. It would be interesting to extend this study to other bombarding conditions and follow the energy dependence of the reaction cross sections. Experiments in this direction are in progress.

This work was supported in part by the Heraeus Foundation and the DFG Grant Bo1109/1.

- 
- [1] *Proceedings of the Workshop on H.I. Collisions at Energies near the Coulomb Barrier*, Daresbury, Great Britain, 1990, edited by M. A. Nagarajan (IOP, Bristol, 1991).
- [2] C. Y. Wu, W. von Oertzen, D. Cline, and M. Guidry, *Annu. Rev. Nucl. Part. Sci.* **40**, 285 (1990).
- [3] R. Künkel, W. von Oertzen, H. G. Bohlen, B. Gebauer, H. A. Bösser, R. Kohlmeyer, J. Speer, F. Pühlhofer, and D. Schüll, *Z. Phys. A* **336**, 71 (1990).
- [4] M. Wilpert, B. Gebauer, W. von Oertzen, Th. Wilpert, E. Stiliaris, and H. G. Bohlen, *Phys. Rev. C* **44**, 1081 (1991).
- [5] K. E. Rehm, A. M. van den Berg, J. J. Kolata, D. G. Kovar, W. Kutschera, G. Rosner, G. S. Stephens, and J. L. Yntema, *Phys. Rev. C* **37**, 2629 (1988).
- [6] A. Winther, *Fizika* **22**, 41 (1990).
- [7] A. Winther, *Nucl. Phys. A* (to be published).
- [8] C. H. Dasso and S. Landowne, *Phys. Lett. B* **183**, 141 (1987).
- [9] P. H. Stelson, *Phys. Lett. B* **205**, 190 (1988).
- [10] H. J. Kim, J. Gomez del Campo, D. Shapira, P. H. Stelson, and D. Napoli, *Phys. Rev. C* **43**, 1321 (1991).
- [11] R. B. Roberts, S. B. Gazes, J. E. Mason, M. Satteson, S. G. Teichmann, L. L. Lee, J. F. Liang, J. C. Mahon, and R. J. Vojtech, *Phys. Rev. C* **47**, R1831 (1993).
- [12] L. Corradi *et al.*, *Z. Phys. A* **334**, 55 (1990).
- [13] L. Corradi *et al.*, *Z. Phys. A* **346**, 217 (1993).
- [14] K. E. Rehm, *Annu. Rev. Nucl. Part. Sci.* **41**, 429 (1991).
- [15] J. Fernandez-Niello *et al.*, *Phys. Rev. C* **45**, 748 (1992).
- [16] K. E. Rehm, B. G. Glagola, W. Kutschera, F. L. H. Wolfs, and A. H. Wuosmaa, *Phys. Rev. C* **47**, R2731 (1993).
- [17] J. F. Liang, L. L. Lee, J. C. Mahon, and R. J. Vojtech, *Phys. Rev. C* **47**, R1342 (1993).
- [18] H. Esbensen and S. Landowne, *Nucl. Phys.* **A492**, 473 (1989).
- [19] J. Thompson, *Comput. Phys. Rep.* **7**, 168 (1988).
- [20] L. Corradi, C. M. Petrache, D. Ackermann, S. Beghini, G. de Angelis, G. Montagnoli, H. Moreno, D. R. Napoli, G. Pollarolo, F. Scarlassara, G. F. Segato, C. Signorini, P. Spolaore, and A. M. Stefanini, *Z. Phys. A* **334**, 353 (1993).
- [21] L. C. Vaz, J. M. Alexander, and G. R. Satchler, *Phys. Rep.* **69**, 374 (1981).
- [22] M. H. Macfarlane and S. C. Pieper, "PTOLEMY: A Program for Heavy-Ion Direct-Reaction Calculations," Report No. ANL-76-11, 1978 (unpublished).
- [23] R. A. Broglia and A. Winther, in *Heavy-ion Reactions* (Addison-Wesley, Redwood City, CA, 1990), Vol. 1, parts I and II.
- [24] D. R. Napoli, A. M. Stefanini, H. Moreno Gonzalez, B. Million, G. Prete, P. Spolaore, M. Narayanasamy, Zi Chang Li, S. Beghini, G. Montagnoli, F. Scarlassara, G. F. Segato, C. Signorini, F. Soramel, G. Pollarolo, and A. Rapisarda, *Nucl. Phys.* **A559**, 443 (1993).
- [25] E. Vigezzi and A. Winther, *Ann. Phys. (N.Y.)* **192**, 432 (1989).
- [26] R. A. Broglia, G. Pollarolo, and A. Winther, *Nucl. Phys.* **A361**, 307 (1981).
- [27] G. Pollarolo, R. A. Broglia, and A. Winther, *Nucl. Phys.* **A406**, 369 (1983).
- [28] C. H. Dasso, S. Landowne, G. Pollarolo, and A. Winther, *Nucl. Phys.* **A459**, 134 (1986).
- [29] C. H. Dasso, G. Pollarolo, and S. Landowne, *Nucl. Phys.* **A443**, 365 (1985).
- [30] C. H. Dasso and G. Pollarolo, *Phys. Lett.* **155B**, 223 (1985).